ORIGINAL PAPER

Electrooxidation of isotope-labeled ethanol: a FTIRS study

M. J. S. Farias · G. A. Camara · A. A. Tanaka

Abstract In this work, we investigated some important aspects related to the electrooxidation of isotope-labeled ethanol on Pt. The central point was the effect of the adsorption potential on the formation of CO_2 produced from both alcohol and methyl groups during the electrooxidation of ethanol in acid media. As a way to follow these contributions, we used isotope-labeled ethanol ($^{13}CH_3CH_2OH$) and Fourier transform infrared spectroscopy (FTIRS). The yield of $^{13}CO_2$ increased with the ethanol adsorption potential. Despite the visualization difficulties due to dipole coupling, ^{13}CO was detected, indicating that the formation of $^{13}CO_2$ follows a mechanism analogous to the one of $^{12}CO_2$.

M. J. S. Farias · A. A. Tanaka (✉)
Departamento de Química, UFMA,
65.085-580 São Luís, Maranhão, Brazil
e-mail: tanaka@ufma.br

G. A. Camara
Instituto de Química de São Carlos, USP,
Caixa Postal 780, 13560-970 São Carlos,
São Paulo, Brazil

Present address:
G. A. Camara
Departamento de Química, UFMS,
C.P. 549, 79070-900 Campo Grande, Mato Grosso do Sul, Brazil

Introduction

Ethanol oxidation reaction has been a subject of permanent interest for many years [1–5]. Its oxidation to CO_2 generates 12 F per mol, which is twice the methanol energy content. Ethanol is a renewable fuel and, therefore, can be considered a potential candidate for fuel cell applications. Additionally, ethanol molecule is the smallest alcohol possessing a C–C bond and can serve as a model to provide information on the oxidation of C–C containing compounds. Specifically, for alcohol molecules, the strength of this bond and its position (generally surrounded by hydrogen from methyl groups) make these chains extremely stable. As a consequence, the complete oxidation of compounds with C–C bonds is a major challenge in electrocatalysis.

Despite the great number of papers devoted to this problem, there is still a lack of electrocatalysts that efficiently promote the breaking of the C–C bond in the ethanol molecule. It is well established that ethanol electrooxidation on Pt in acid solution occurs via parallel reactions that produce mainly acetaldehyde and acetic acid and minor amounts of CO_2. Thus, in addition to the low energy yield, undesirable products are accumulated [5].

In this context, the use of $^{13}CH_3CH_2OH$ makes it possible to distinguish the behavior of both C-atoms of the original alcohol molecule and to gain some knowledge about the reaction mechanism. A central point would be: We already know that CO_2 is unequivocally formed from the $–CH_3$ group, but the question is, to what extent does $^{13}CO_2$ contributes to the total amount of CO_2 produced during the electrooxidation of ethanol? Thus, this work presents new experimental spectroscopic results to gain a better understanding on this subject.

Materials and methods

The working electrode was a smooth polycrystalline Pt disk with a geometric surface area of 0.78 cm^2. The real surface area value was determined as ∼0.94 cm^2, by integration of the charge in the hydrogen region of the cyclic voltammogram, and used in the calculation of the current densities. The counter electrode was a 1.2-cm^2 platinum sheet. All potentials were measured against a reversible hydrogen electrode in the supporting electrolyte; the latter was HClO$_4$ 0.1 M (Aldrich® 99.99%).

Before each experiment, the Pt disk was flame-annealed for 10 min and cooled in argon atmosphere. The electrode was immediately transferred to the electrochemical cell containing 0.1 M HClO$_4$. The state of the electrode surface was checked by running a cyclic voltammogram between 0.05 and 1.45 V at 20 m V s^{-1}, with the electrode in meniscus configuration. Then, the potential was kept at 0.05 V and ethanol (J. T. Baker) added into the cell to obtain the desired concentrations.

The solutions were prepared with Milli-Q water (18.2 MΩ cm) and deaerated with N$_2$ (analytical grade, 4.6). All experiments were performed at room temperature (25±1.0 °C).

The Fourier transform infrared spectroscopy (FTIRS) experiments were performed with a Nicolet Nexus 670 spectrophotometer, and the spectroelectrochemical cell used is described in detail elsewhere [6]. The cell was fitted with a prismatic 60° CaF$_2$ window. Spectra were obtained from the average of 16 interferograms using a resolution of 8 cm^{-1}. Under these conditions, each spectrum was measured at about 6.5 s. Reflectance spectra were calculated as the ratio (R/R_o) where R represents a spectrum at the sample potential and R_o a spectrum collected at 0.05 V. For the experiments varying with the adsorption potential, reference spectra were also taken at 0.1, 0.2, or 0.3 V. Positive and negative bands represent, respectively, the consumption and production of species at the sample potential.

From the integrated band intensities, A_i, for $^{12}CO_2$ and $^{13}CO_2$ (2,340 cm^{-1} and 2,274 cm^{-1}, respectively) and the effective absorption coefficient (ε_{eff}), the respective molar amounts (Q_i, mol/cm^2) were calculated using the relation [1, 4]:

$$Q_i = A_i / \varepsilon_{eff}. \tag{1}$$

Results and discussion

Voltammetric results

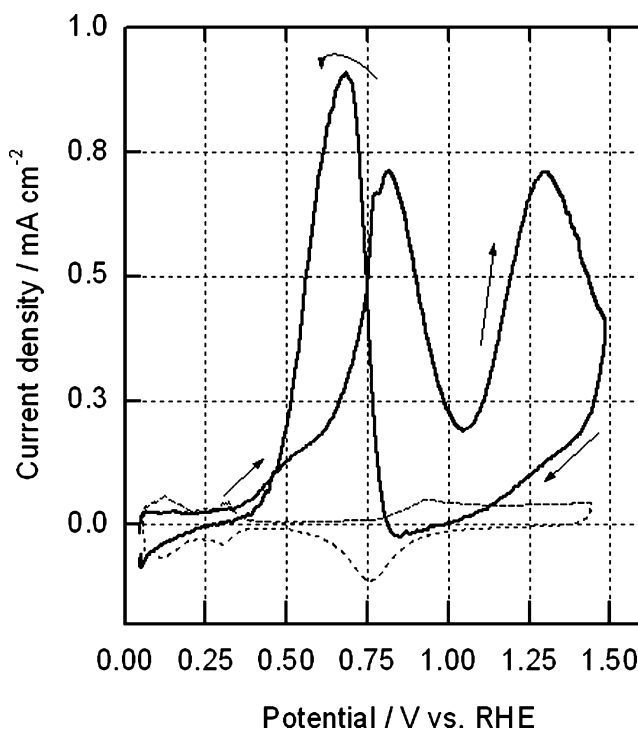Figure 1 shows the first scan of a cyclic voltammogram recorded at 20 mV s^{-1} on the polycrystalline Pt electrode in a solution containing 0.1 M ethanol in 0.1 M HClO$_4$. The solution was prepared by adding ethanol into the cell containing the supporting electrolyte with the working electrode polarized at 0.05 V. For ends of comparison, a CV with Pt in HClO$_4$ is also shown (dotted line).

The voltammogram shows the well-established pattern of other small organic molecules. A blockage of Pt sites indicates that the adsorption of ethanol occurs at the initial potential of 0.05 V, as will be discussed below. During the positive-going scan, a small electrode activity is observed between 0.35 and 0.55 V. At the latter potential, a pronounced increase in current occurs, forming peaks at 0.81 V (first peak) and 1.30 V (second peak). During the negative-going scan, a reactivation of the electrode surface occurs, producing a unique peak at about 0.68 V.

As to monitoring the potential dependence of the oxidation products, in situ FTIR spectra were measured, and the results are presented in the next section.

Spectroscopic results—the effect of the potential

Figure 2 shows in situ FTIR spectra obtained in 0.1 M ethanol + 0.1 M HClO$_4$ solution, after a series of potential steps. Initially, a reference spectrum R_o was measured at 0.05 V, and then, sample spectra were collected after

Fig. 1 *Solid line* First scan of a cyclic voltammogram experiment for ethanol electrooxidation on smooth polycrystalline Pt electrode in 0.1M HClO$_4$ solution containing 0.1 M ethanol. *Dotted line* Cyclic voltammogram of the Pt electrode in 0.1 M HClO$_4$. T=25 °C, v= 20 mV s^{-1}
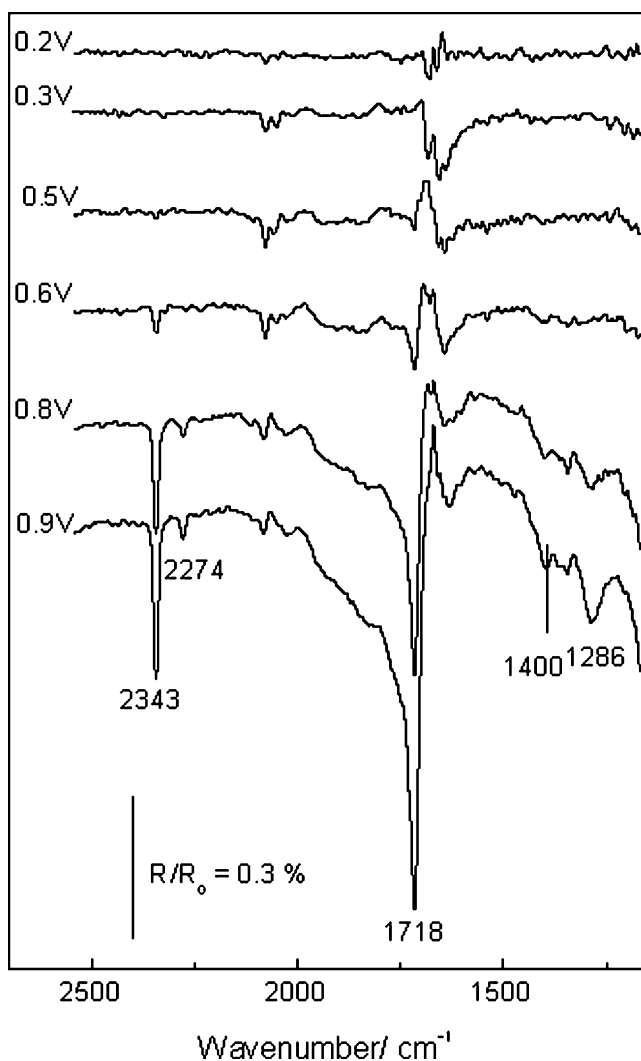
Fig. 2 In situ FTIR spectra recorded at different potentials for a smooth Pt electrode in 0.1 M ethanol + 0.1 M $HClO_4$ solution, 0.1–0.9 V. Reference spectra taken after 15 min of polarization at 0.05 V. Sample spectra measured after application of successive potential steps of 50 mV. Spectra averaged from 16 scans

applying successive potential steps of 0.05 V up to a potential of 1.4 V. Results show spectra comprised between 0.2–0.9 V. The most important features related to ethanol oxidation products are marked in the figure. For a more complete assignment of the bands in the region comprised between 2,030 and 1,280 cm^{-1}, see [7]. Figure 2 shows that, already at 0.2 V, a band centered at ~2,030 cm^{-1}, ascribed to linearly adsorbed C-12 carbon monoxide ($^{12}CO_L$) [8], can be noted. The production of CO indicates that dissociative adsorption of ethanol is already taking place at this potential. The CO_L intensity band grows up to a potential of 0.5 V, where a very weak band corresponding to the production of $^{12}CO_2$ is observed. At this scale, only a very weak ^{13}CO corresponding band (~1,960 cm^{-1}) can be observed; details on the development of this band will be discussed later.

It can be noted that, in addition to the $^{12}CO_2$ band (2,343 cm^{-1}), a weaker feature at 2,274 cm^{-1}, ascribed to $^{13}CO_2$ [9], starts to grow at 0.8 V. Further details on the dependence of the band intensities with the potential are presented in Fig. 3. Figure 2 also shows that bands relative to the production of a carboxylic acid (1,286 and 1,400 cm^{-1} [10], generally attributed to acetic acid) and carbonyl-containing species (1,718 cm^{-1} [9]) begin to grow at potentials above 0.6 V, as found on a previous paper [5]. However, it is necessary to take into account that both bands at 1,286 and 1,400 cm^{-1} are not unequivocally specific of acetic acid. For instance, Pettersson et al. [11] have attributed these bands to formic acid. Thus, at this point, we cannot discard such possibility, although there is no evidence that formic acid can be formed from CO groups under such conditions.

Figure 3 show molar amounts relative to $^{12}CO_2$ and $^{13}CO_2$ as a function of the potential for a 0.1 M ethanol + 0.1 M $HClO_4$ solution. These values where obtained by conversion of the integrated band intensities in molar amounts by using the effective absorption coefficients calculated by Weaver et al. [1, 4]. Values of ε_{eff} were assumed to be 3.5×10^4 M^{-1} cm^{-2} for both $^{12}CO_2$ and $^{13}CO_2$.

An important remark in the foregoing discussion is that the $^{12}CO_2$ band intensity is significantly higher than the $^{13}CO_2$ one for all investigated potentials. This result is consistent with those ones obtained by Shin et al. [9]. These authors have investigated the catalytic performance of Pt (111) and (335) towards the oxidation of isotopic-labeled ethanol. They found a minor production of CO_2 from –CH_3 group at potentials above the hydrogen adsorption region [9]. Further details about the distinct dependence of $^{13}CO_2$
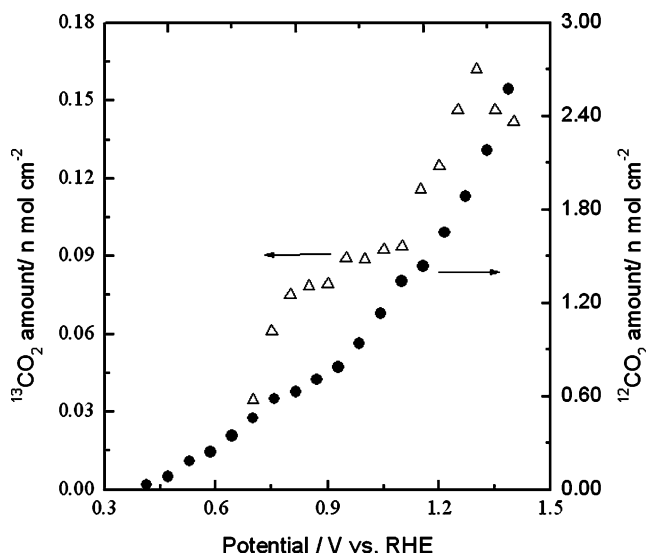
Fig. 3 Amounts of (*open triangle*) $^{13}CO_2$ and (*filled circle*) $^{12}CO_2$ obtained after successive 50 mV potential steps in 0.1 M ethanol + 0.1 M $HClO_4$ solution. Data extracted from Fig. 2

and $^{12}CO_2$ are being analyzed at the moment and will be presented in due course.

Despite the intrinsic difficulty to correlate potentiodynamic data (obtained from CVs) with in situ FTIR experiments, where potential steps were applied in a thin layer configuration [12], analyses in Figs. 2 and 3 put some highlights on the behavior of the cyclic voltammogram shown in Fig. 1:
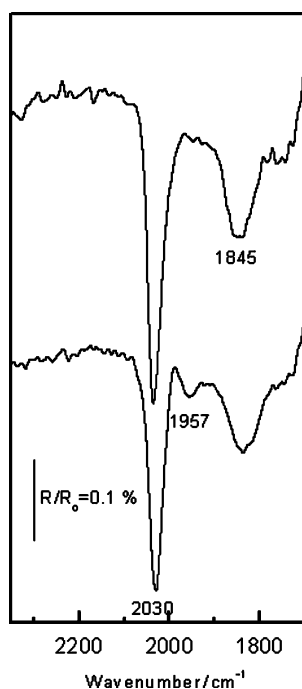
1. The onset potential for $^{12}CO_2$ formation is about 0.5 V, coinciding with the pre-peak in the voltammogram.
2. The production of acetic acid is followed by a corresponding increase of current in the CV.

Aiming at gaining further knowledge about the dissociative adsorption of ethanol taking place on Pt surface and forming CO, the productions of linear CO ($^{12}CO_L$, $^{13}CO_L$) and bridge-bonded CO (CO_B) were accompanied by FTIR in situ, and the results are presented in the next section. CO_B was considered as a single species, as it was not possible to separate signals corresponding to $^{12}CO_B$ and $^{13}CO_B$.

The presence of ^{13}CO

Figure 4 shows FTIRS spectra obtained at 0.35 V in a 0.25 M ethanol solution for regular- (upper curve) and isotopic-labeled ethanol (lower curve). In both cases, the spectra were calculated using a reference spectrum taken at 0.05 V. Fig. 4 shows that when $^{12}CH_3CH_2OH$ is replaced by $^{13}CH_3CH_2OH$, in addition to the presence of CO_L (2,030 cm^{-1}) and CO_B (1,845 cm^{-1}), a third CO band

Fig. 5 FTIRS spectra obtained at 0.7 V in 0.1 M ethanol + 0.1 M HClO$_4$ solution at different adsorption potentials (E_{ad}), as indicated in the figure. Before the acquisition of spectra, the electrode was maintained at such potentials for 15 min
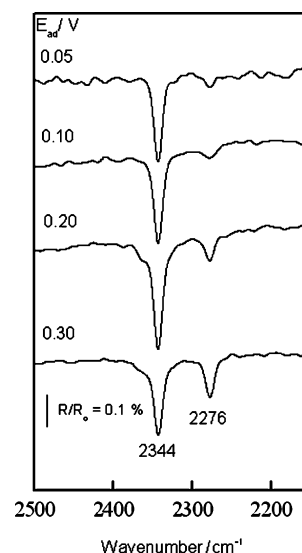
(1,957 cm^{-1}) becomes apparent. This band is attributed to ^{13}CO, and its low intensity is partially caused by a dipole coupling and intensity sharing causing the lowering of ^{13}CO and the dominance of the ^{12}CO band [9, 13, 14]. This effect is particularly pronounced at high surface coverages [8], as we have also observed. Despite the impossibility of using CO bands for quantitative purposes, the relevance of the results presented in Fig. 4 cannot be ignored because they indicate that at least part of the $^{13}CO_2$ produced at high potentials is preceded by dehydrogenation steps of $^{13}CH_3$ at low potentials (below 0.35 V).
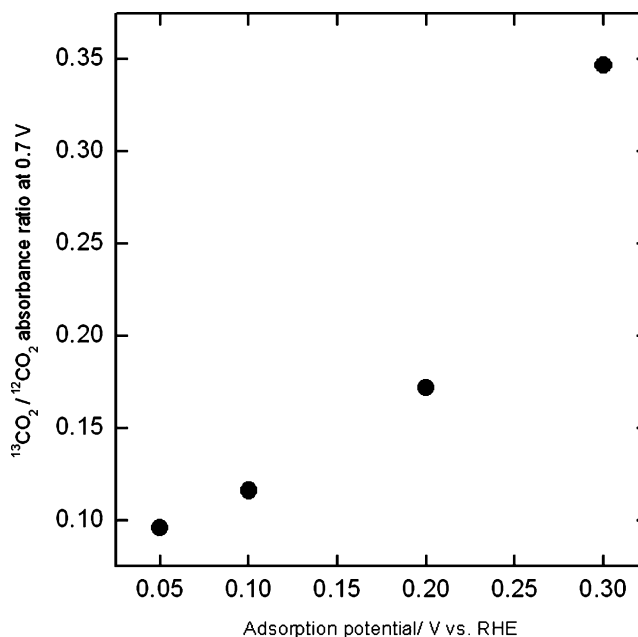

Fig. 4 FTIRS spectra obtained at 0.35 V in a 0.25 M ethanol + 0.1 M HClO$_4$ solution for $^{12}CH_3CH_2OH$ (upper curve) and $^{13}CH_3CH_2OH$ (lower curve). Reference spectra taken at 0.05 V

Fig. 6 Ratio $^{13}CO_2/^{12}CO_2$ obtained at 0.7 V as a function of the adsorption potential Data calculated from spectra in Fig. 5

The influence of the adsorption-potential

Figure 5 shows spectra obtained at 0.7 V for a 0.1 M ethanol solution at different potentials of adsorption, namely, 0.05, 0.10, 0.20, and 0.30 V vs RHE. Before the acquisition of spectra, the electrode was maintained at such potentials for 15 min. For a better visualization of $^{12}CO_2$ and $^{13}CO_2$ bands (at 2,344 and 2,276 cm^{-1}, respectively), only the region comprised between 2,500 and 2,150 cm^{-1} is shown. This potential was chosen because it is the lowest where the intensity of the 2,276-cm^{-1} band is enough to allow the integration of its area. It should be noted that the production of $^{12}CO_2$ is almost not affected by the adsorption potential. On the other hand, $^{13}CO_2$ formation is clearly favored when the adsorption potential is increased from 0.05 up to 0.30 V. The ratio of $R = {}^{13}CO_2/{}^{12}CO_2$ at 0.7 V as a function of the adsorption potential is shown in Fig. 6. The value of R is around 0.1 when ethanol is adsorbed at 0.05 V, indicating that $^{13}CO_2$ contribution for global CO_2 is very small. R increases with the adsorption potential, reaching 0.35 when ethanol is adsorbed at 0.3 V.

A similar trend was earlier reported from data obtained by on-line differential electrochemical mass spectrometry (DEMS) and in situ FTIRS [3]. When the adsorption occurs at low potentials (e.g., 0.05 V), a significant fraction of –CH$_3$ is reduced to CH$_4$ and, in a minor extent, to C$_2$H$_6$. As a consequence, part of the adsorbate from ^{13}CH$_3$ group is lost at the low potentials [3].

According to Cattaneo et al. [15], the same quantity of $^{13}CO_2$ and $^{12}CO_2$ is obtained by DEMS when ethanol is adsorbed at 0.4 V. The explanation for this fact is that when the adsorption of ethanol is performed at such potential its reduction to hydrocarbons is prevented.

Conclusions

- $^{13}CO_2$ is only produced at higher potentials than those observed for $^{12}CO_2$. Such difference seems to be associated with a major difficulty to oxidize CH$_3$ groups.
- ^{13}CO is formed through –CH$_3$ group from the ethanol molecule. Despite the impossibility to quantify ^{13}CO, due to dipole coupling effects, its presence, during the electrooxidation of the isotope-labeled ethanol, is an unequivocal proof that the pathway towards $^{13}CO_2$ has ^{13}CO as intermediate species.
- When the adsorption of ethanol occurs at low potentials (e.g., 0.05 V), a significant fraction of –CH$_3$ is reduced to CH$_4$ and, in a minor extent, to C$_2$H$_6$. On the other hand, for adsorption at potentials above the hydrogen region, the reduction to hydrocarbons is prevented, and the $^{13}CO_2$ formation is favored.

References

1. Leung L-WH, Chang S-C, Weaver MJ (1989) J Electroanal Chem 266:317
2. Xia XH, Liess HD, Iwasita T (1997) J Electroanal Chem 437:233
3. Iwasita T, Pastor E (1994) Electrochim Acta 39:53
4. Gao P, Chang S-C, Zhou Z, Weaver MJ (1989) J Electroanal Chem 272:161
5. Camara GA, Iwasita T (2005) J Electroanal Chem 578:315
6. Iwasita T, Nart FC (1997) In: Gerischer H, Tobias CW (eds) In-situ infrared Fourier transform spectroscopy: a tool to characterize the metal-interface at a molecular level. Advances in electrochemical science and engineering, vol 4. Wiley-VCH, New York, pp 123–216
7. Shao MH, Adzic RR (2005) Electrochim Acta 50:2415
8. Bewick A, Kunimatsu K, Pons S (1980) Electrochim Acta 25:465
9. Shin J, Tornquist WJ, Korzeniewski C, Hoaglund CS (1996) Surf Sci 364:122
10. Socrates G (1966) Infrared characteristic group frequencies. Wiley, New York
11. Pettersson M, Lundell J, Khriachtchev L, Rasanen M (1997) J Am Chem Soc 119:11715
12. Nart FC, Iwasita T (1997) Prog Surf Sci 55:271
13. Hayden BE (1987) In: Madey TE and Yates JT Jr (eds) Reflection-absorption infrared spectroscopy. Vibrational spectroscopy of molecules on surfaces (methods of surface characterization). Kluwer, New York
14. Hollins P, Pritchard J (1985) Prog Surf Sci 19:275
15. Cattaneo BB, Wilhelm S, Buschmann HW, Vielstich (1988) Ber Bunsenges Phys Chem 92:1210